Routledge
Taylor & Francis Group

Journal of Sports Sciences

ISSN: (Print) (Online) Journal homepage: www.tandfonline.com/journals/rjsp20

Validation of LEOMO inertial measurement unit sensors with marker-based three-dimensional motion capture during maximum sprinting in track cyclists

Roné Thompson, Rodrigo Rico Bini, Carl Paton & Kim Hébert-Losier

To cite this article: Roné Thompson, Rodrigo Rico Bini, Carl Paton & Kim Hébert-Losier (05 Mar 2024): Validation of LEOMO inertial measurement unit sensors with marker-based three-dimensional motion capture during maximum sprinting in track cyclists, Journal of Sports Sciences, DOI: 10.1080/02640414.2024.2324604

To link to this article: https://doi.org/10.1080/02640414.2024.2324604

Published online: 05 Mar 2024.

JOURNAL OF SPORTS SCIENCES
https://doi.org/10.1080/02640414.2024.2324604

Routledge
Taylor & Francis Group

SPORTS MEDICINE AND BIOMECHANICS

Validation of LEOMO inertial measurement unit sensors with marker-based three-dimensional motion capture during maximum sprinting in track cyclists

Roné Thompson [a,b], Rodrigo Rico Bini[c], Carl Paton[d] and Kim Hébert-Losier[a]

[a]Division of Health, Engineering, Computing and Science, Te Huataki Waiora School of Health, University of Waikato, Adams Centre for High Performance, Tauranga, New Zealand; [b]Department of Performance Health, High Performance Sport New Zealand, Grassroots Trust Velodrome, Cambridge, New Zealand; [c]Rural Health School, La Trobe University, Victoria, Australia; [d]School of Health and Sport Science, Te Pukenga at Eastern Institute of Technology, Napier, New Zealand

ABSTRACT

LEOMO™ is a commercial inertial measurement unit system that provides cycling-specific motion performance indicators (MPIs) and offers a mobile solution for monitoring cyclists. We aimed to validate the LEOMO sensors during sprint cycling using gold-standard marker-based three-dimensional (3D) motion technology (Qualisys, AB). Our secondary aim was to explore the relationship between peak power during sprints and MPIs. Seventeen elite track cyclists performed 3 × 15s seated start maximum efforts on a cycle ergometer. Based on intraclass correlation coefficient ($ICC_{3,1}$), the MPIs derived from 3D and LEOMO showed moderate agreement (0.50 < 0.75) for the right foot angular range (FAR); left foot angular range first quadrant (FARQ1); right leg angular range (LAR); and mean angle of the pelvis in the sagittal plane. Agreement was poor (ICC < 0.50) between MPIs derived from 3D and LEOMO for the left FAR, right FARQ1, left LAR, and mean range of motion of the pelvis in the frontal and transverse planes. Only one LEOMO-derived (pelvic rotation) and two 3D-derived (right FARQ1 and FAR) MPIs showed large positive significant correlations with peak power. Caution is advised regarding use of the LEOMO for short maximal cycling efforts and derived MPIs to inform peak sprint cycling power production.

ARTICLE HISTORY
Received 25 March 2023
Accepted 22 February 2024

KEYWORDS
Cycling; kinematics; ergometer; inertial measurement unit; three-dimensional motion capture

Introduction

Many practitioners and researchers capture biomechanics in clinics and laboratories attempting to enhance performance or mitigate injury risk. In cycling, most studies evaluating cycling biomechanics and the optimal cycling positions are based on sub-maximal tests, making the outcomes mainly applicable to road cyclists (R. R. Bini et al., 2016; Galindo-Martinez et al., 2021; Geoffrey et al., 2020). In sports, it is important to assess athletes in their sporting environment and undertake naturalistic research (Bishop, 2008; Williams & Kendall, 2007), which for track cyclists, would involve gathering kinematics and kinetic data on the velodrome track.

Unfortunately, using gold standard three-dimensional (3D) motion analysis to analyse kinematics on the velodrome is challenging due to high costs, considerable time requirements, and a low number of recorded cycles due to the stationary position of cameras on a small section of the track (Bernardina et al., 2019). Although kinetic analysis is possible on a track through high-quality power metres, obtaining these data on the track is more challenging than within a controlled laboratory environment (H. A. Ferguson et al., 2021). Therefore, kinematic and kinetic data from sprint cyclists are typically obtained in laboratory on a cycle ergometer (Burnie, 2020; Burnie et al., 2023; Nimmerichter & Williams, 2015). However, cycling on a cycle ergometer differs from actual cycling conditions (Bertucci et al., 2005) or cycling on a track (Brito et al., 2014; Burnie, 2020; Nimmerichter & Williams, 2015), plausibly due to less technical ability (Nimmerichter & Williams, 2015) and less stabilisation required on an ergometer (Burnie, 2020). Several approaches and tools can be used to measure posture or kinematics of cyclists on their bikes, which may cause discrepancies in outcomes (R. Bini et al., 2023). Various tools are available to quantify motion, including two-dimensional (2D) videos, gold-standard 3D marker-based motion analysis systems, electrogoniometers and inertial measurement units (IMUs) (R. Bini et al., 2023; Fonda et al., 2014). Some researchers recommend using 3D above 2D for assessing lower extremity kinematics during cycling due to the greater precision (Fonda et al., 2014; Pouliquen et al., 2020).

Nonetheless, IMUs are a wearable technology becoming popular in sports (Benson et al., 2022; Hughes et al., 2021) that typically incorporate tri-dimensional linear accelerometers, magnetometers, and gyroscopes (Hughes et al., 2021). IMUs can record large quantities of kinematic data in sport (Van der Kruk & Reijne, 2018) outside of laboratories, increasing ecological validity (Hughes et al., 2021). It may be a valid and more cost-effective alternative to 3D analyses (Hughes et al., 2021) and is already used in different individual and team sports (Chambers et al., 2015), such as tennis (Brocherie & Dinu, 2022; Delgado-García et al., 2020), running (Benson et al., 2022; Picerno, 2017; Routhier et al., 2020), basketball (Slawinski et al., 2018), and snow sports (Chambers et al., 2015).

IMUs also have limitations, with sensor selection needing careful consideration and being chosen based on technical

CONTACT Roné Thompson rt275@students.waikato.ac.nz Division of Health, Engineering, Computing and Science, Te Huataki Waiora School of Health, University of Waikato, Adams Centre for High Performance, Tauranga 3116, New Zealand

specifications and requirements (Hughes et al., 2021). The LEOMO™ motion sensor system (TYPE-S, LEOMO, Boulder, Co, USA) is an IMU system used within the running and cycling community (Millour et al., 2022; Plaza-Bravo et al., 2022). It has shown excellent to moderate validity in computing the range of lower extremity motion in the sagittal plane during steady-state cycling in a laboratory, but the presence of systematic errors in measuring angular range of leg motion and pelvic angles (Plaza-Bravo et al., 2022). LEOMO sensors are quick, easy (LEOMO Help Centre, 2020a) and non-invasive to place and could allow data to be captured during sprint starts and continuously in a velodrome if shown valid for this particular purpose. Such information may not only support the optimisation of performance (e.g., aerodynamic position on the bike) (Faulkner & Jobling, 2021), but also the management of injuries (e.g., positions on the bike that reduce pain or progression of pathologies) (Frank et al., 2018; Wadsworth & Weinrauch, 2019).

The LEOMO system outputs motion performance indicators (MPIs) for cyclist, such as angular range and pelvic angle. Although there is limited research on the MPIs as defined by the manufacturer, the relationship between MPIs and performance in professional cyclists has been explored during a graded exercise test performed on a cycle ergometer. An increase pelvic inclination and rotation was observed at higher intensities and reduced right foot range of movement (ROM) was moderately associated with greater peak power (Courel-Ibáñez et al., 2021). Given the existing research on the LEOMO system in road cycling (Courel-Ibáñez et al., 2021; Plaza-Bravo et al., 2022), we aimed to validate the MPIs derived from the LEOMO TYPE-S against gold-standard 3D analysis with elite track cyclists performing seated maximum sprinting in a laboratory and hypothesis this system would be valid. Provided the potential link between cycling kinematics and performance, a secondary aim was to investigate the possible relationship between the MPIs described by the LEOMO system and peak power output in elite track sprint cyclists. We hypothesised that there would be a relationship between the MPIs and peak power.

Materials and methods

Sample size

The sample size was calculated based on correlation coefficients from a prior validation study on the LEOMO device, where an average correlation coefficient of $r = 0.694$ between LEOMO and 2D motion data was reported (Plaza-Bravo et al., 2022). On that basis, 14 cyclists were required when calculating sample size requirements using an online calculator (https://sample-size.net/correlation-sample-size/), setting α at 0.05 and β at 0.20 (Hulley et al., 2013; Lachin, 1981). The Human Research Ethics Committee approved the study before participant recruitment.

Participants

To be included, cyclists needed to be elite track cyclists, competing at competitions sanctioned by the Union Cycliste Internationale (Phillips & Hopkins, 2020). Cyclists who had current injuries or illnesses were excluded. Nineteen sprint track cyclists (team sprint, 500 to 1000-m time trial, match sprint, and Keirin riders) (H. Ferguson et al., 2023) were recruited through flyers and personal communications to Cycling New Zealand, although two did not meet inclusion criteria. According to the Union Cycliste Internationale classification, eleven were elite cyclists (8 males, 3 females) embedded full-time into the national track cycling program, and six were elite junior cyclists (U/19) (Phillips & Hopkins, 2020) (Table 1). All cyclists provided written informed consent and were informed of the risks and benefits associated with the study, mainly delayed onset muscle soreness and individualised reports, respectively.

Protocol

Cyclists attended a single data collection session at the national training centre. Cyclists attached their track bikes (see Gear in Table 1) to a Wahoo cycle ergometer KICKR smart trainer (Wahoo Fitness, LLC, Atlanta, USA). Cyclists wore their own cycling shoes and training gear for testing. The KICKR measures power to a comparable level of accuracy to the SRM power metres during incremental exercise testing, with a mean typical error of measurement of 1.5% versus 0.7% for the SRM (Hoon et al., 2016).

Cyclists completed a self-directed 10–15-minute warm-up prior to testing. Afterwards, the same experienced physiotherapist affixed 45 retro-reflective markers (12.5 mm in diameter) to the skin and shoes of cyclists using adhesive tape based on the Calibrated Anatomical System Technique (Cappozzo et al., 1997; Hébert-Losier et al., 2019). The 45-marker model included five clusters to minimise the effect of skin movement artefacts (Benoit et al., 2006). All 45 markers (bilaterally on the anterior superior iliac spine, posterior superior iliac spine, greater trochanter, medial and lateral femoral epicondyle**s**, medial and lateral malleoli, medial forefoot, acromioclavicular joint,

Table 1. Characteristics (mean ± SD) of cyclists recruited ($n = 17$) and their bikes used in the three 15-s maximal sprint efforts, as well as peak power and peak cadence from the best 15-s effort.

	Elite ($n = 11$)		U19 Elite ($n = 6$)	
	M ($n = 8$)	F ($n = 3$)	M ($n = 3$)	F ($n = 3$)
Age (y)	24.8 ± 3.0	22.4 ± 1.3	18.8 ± 1.2	17.4 ± 0.6
Mass (kg)	84.5 ± 7.0	71.4 ± 8.7	72.3 ± 6.4	60.0 ± 7.0
Height (m)	1.83 ± 0.08	1.69 ± 0.08	1.80 ± 0.06	1.67 ± 0.02
Gear (inches)	104	98	98	98[a], 96[b]
Peak power (watts)	1332.5 ± 132.6	982.0 ± 82.6	899.3 ± 137.2	736.0 ± 130.3
Peak cadence (rpm)	112.9 ± 5.0	109.7 ± 2.5	112.7 ± 4.9	99.0 ± 7.9

[a]Two cyclists. [b] One cyclist. Abbreviations: F = female; M = male; SD = standard deviation; U19 = under 19.

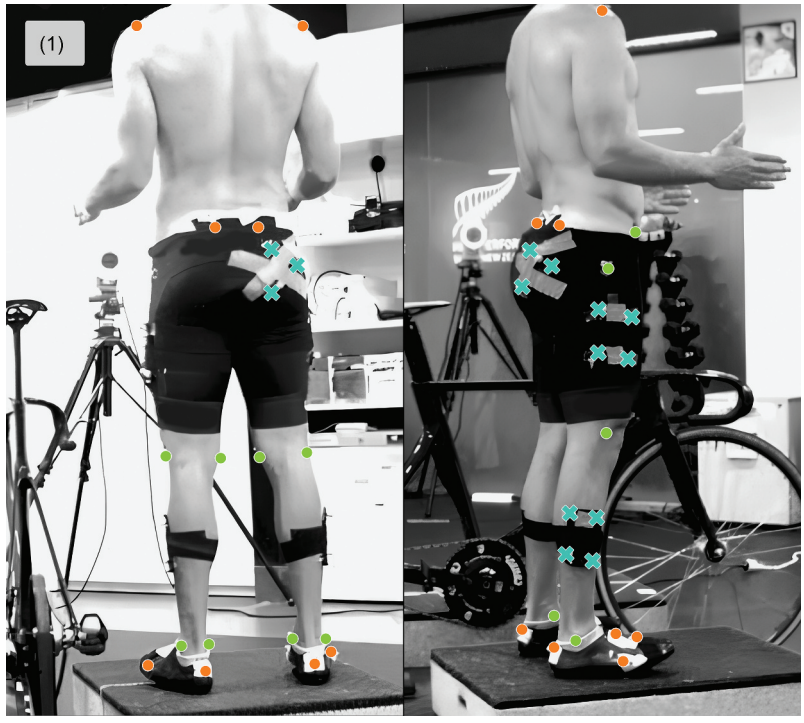

Figure 1. Position of the 45 retro-reflective markers (posterior and lateral views). The green circle markers were removed after the static trial; the clusters (crosses) and orange circle markers stayed on the participant during testing.

posterior heel, superior midfoot, fifth metatarsal, inferior midfoot, thigh four-marker cluster, and shank four-marker cluster; and unilaterally on the right pelvis three-marker cluster were used for static calibration in standing, with 14 markers removed for the on-bike seated dynamic trials, as shown in Figure 1.

The physiotherapist also placed the five Type-S LEOMO motion sensors (Type-S Motion Sensor, Leomo, Inc., Boulder, Colorado, USA) using adhesive tape according to the manufacturer's instructions (LEOMO Help Centre, 2020b), as shown in Figure 2.

For testing, cyclists completed 3×15 seconds of maximal efforts starting from stationary. Cyclists were required to remain seated during the efforts and aim to reach a cadence between 80–120 rpm. Cyclists had a 5-minute passive recovery between repetitions, staying seated on their bikes. Before the three maximal efforts, cyclists completed 1×15s at 30–50% of maximum effort to assist with familiarisation. After data collection, cyclists completed a self-directed cooldown. All cyclists were familiar with using a cycle ergometer trainer as part of their regular training.

Data collection

During the three 15 s maximal cycling efforts, power data from the same Wahoo cycle ergometer were sampled at 1 Hz via Bluetooth using the Wahoo application on an Apple iPhone XR iOS 15.4 (Apple Inc). Marker data were recorded at 200 Hz using an 8-camera 3D motion capture system (Oqus 700+ cameras)

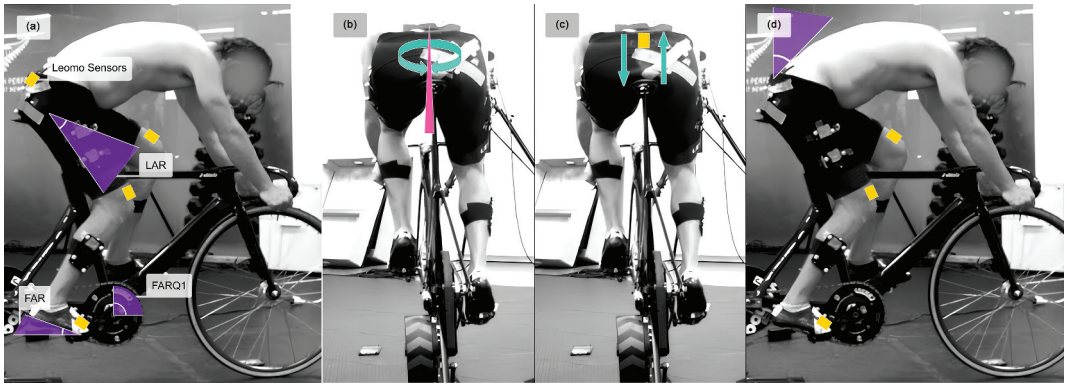

Figure 2. Positioning of the five type-S LEOMO sensors (yellow rectangles) and schematic representation of the derived motion performance indicators (MPIs). (a) Lower limb MPIs: leg angular range (LAR), foot angular range (FAR), foot angular range first quadrant (FARQ1). (b) Pelvic rotation MPI: mean range of motion of the pelvis in the transverse plane (right-left around the vertical axis). (c) Pelvic rocking MPI: mean range of motion of the pelvis in the coronal plane (superior-inferior around the anterior-posterior axis). (d) Pelvic angle MPI: mean angle of the pelvis in the sagittal plane (anterior-posterior around the medial-lateral axis).

and software (Qualisys Track Manager v.2021 release 6470, Qualisys AB, Gothenburg, Sweden). The LEOMO sensor data were simultaneously collected at 100 Hz via wireless technology using a Live Video Synchronisation application on an Apple iPad Pro 10th generation iOS 15.4 (Apple Inc). The processed data from the LEOMO device were obtained from the LEOMO web application in.csv format (http://app.leomo.io).

Data processing

Peak power (W) over one second were extracted from the Wahoo cycle ergometer from each one of the 15 s cycling trials. Any missing 3D marker data up to 10 frames were gap-filled within the Qualisys Track Manager software using cubic polynomial interpolation. Marker data were exported to the.c3D format and converted to TRC files using bespoke scripts in MATLAB (R2022a; MathWorks, Natick, MA, USA). A generic musculoskeletal model (Catelli et al., 2019) was customised for increased hip and knee angles (Full Body Model to Perform Deep Squatting and High Hip Flexion Task) and applied to the collected data. The model was scaled for each participant using the static trial followed by inverse kinematics in OpenSim 4.4 (Delp et al., 2007). The maximum marker errors were less than 1.6 cm for all reconstructions, meeting OpenSim best practice recommendations. Segment orientations for the pelvis, feet, and thighs, as well as joint angles based on Euler angle, were extracted and used to calculate the following MPIs, consistent with the key outputs from LEOMO: Foot Angular Range (FAR) – foot angular range of motion; Foot Angular Range first quadrant (FARQ1) – foot angular range of motion for the propulsive phase of the crank cycle, 12 o'clock to 3 o'clock position; Leg Angular Range (LAR) – angular range of motion for the upper leg (i.e., thigh); Pelvic Angle – mean angle of the pelvis in the sagittal plane (anterior – posterior) in relation to vertical; Pelvic Rock – mean range of motion of the pelvis in the coronal plane (superior – inferior); and Pelvic Rotation – mean range of motion of the pelvis in the transverse plane (right – left). To synchronise the data between the 3D and LEOMO systems, we identified the cycle through peak cadence and extracted the data from the five crank cycles immediately preceding peak cadence. In Opensim, the peak acceleration of the feet derived from the foot centre of mass was used to define crank cycles, where peak acceleration indicated the bottom dead centre. This method was used to replicate the description of crank cycle identification provided by the LEOMO manufacturer. The LEOMO data were obtained from the processed.csv file delivering data at a sampling rate of one second (i.e. average 1-second data). MATLAB was then used to extract the nine MPIs from both the 3D and LEOMO systems from the same five pedal cycles. The pelvic angle orientation in the sagittal plane was standardised between the two systems, where a pelvic angle of 0° represents the pelvis being vertical and 90° being horizontal.

Statistical analysis

Statistical analysis for the primary aim of validating the LEOMO sensors with the 3D motion was performed on the data from the 17 cyclists using the trial generating the greatest peak power for each cyclist. An extreme studentised deviation (Grubbs' test) was applied to all the 3D and LEOMO data using the Prism software (GraphPad Prism 9.1) to identify whether the most extreme values were significant outliers. One data point was removed from all the 3D MPIs due to being a significant outlier for seven of the nine indicators ($p < 0.05$); hence, analysis was performed on data from 16 participants. The reason for the outlying data was deemed the result of hair and clothing covering 3D markers. One data point was removed from the LEOMO dataset since the left LAR sensor failed to collect data, resulting in data from 15 cyclists available to analyse that specific MPI.

All data were assessed for normality of distribution using the Shapiro-Wilk test and passed normality assumptions, except the LEOMO right LAR MPI ($p = 0.047$) and the 3D data of the pelvic rotation ($p = 0.020$). As most of the data were normally distributed, parametric testing was used. Data were summarised using means and standard deviations (mean ± SD). Intraclass correlation coefficient ($ICC_{3,1}$) and 95% confidence interval [lower, upper] were extracted using a statistical spreadsheet to assess the relative agreement between the 3D and LEOMO data (Hopkins, 2015). Based on typical thresholds, ICC values of less than 0.50, between 0.50 and 0.75, between 0.75 and 0.90, and greater than 0.90 were deemed indicative of poor, moderate, good, and excellent agreement, respectively (Koo & Li, 2016; Portney, 2020). Furthermore, Bland-Altman scatterplots with the mean bias and 95% limits of agreement (mean difference ±1.96 standard deviations) were constructed (Bland & Altman, 1999). If data presented as homoscedastic, linear regression analysis was performed and presented on the Bland and Altman graphs.

For the secondary aim of exploring the relationship between cycling kinematics and peak power output, data were taken from trials with the highest and lowest recorded peak power output. All data were again assessed for normality of distribution, which revealed that one of the nine 3D MPIs (sagittal plane pelvic angle) and three of the nine LEOMO MPIs (right LAR, left FAR and left FARQ1) presented non-normal distributions. Given most of the data were normally distributed and to maintain consistency, parametric approaches consisting of Pearson correlations and linear regressions were used to explore the relationship between change in peak power output and change in MPIs. Thresholds of r values of 0.10, 0.30 and 0.50 were used to indicate small, medium, and large correlations, respectively (Cohen, 1992). The significance level was $p \leq 0.05$ for all analyses performed using Microsoft® Excel® (Office 365 M) and GraphPad Prism 9.1.

Results

Validity and Bland-Altman plots

Peak power and cadence from the best trials of cyclists are shown in Table 1. Descriptive and validity statistics for the MPIs are presented in Table 2. There was poor relative agreement between the two systems for the MPIs of left FAR, right FARQ1, left LAR, pelvic rock, and pelvic rotations (ICC <0.50). At best, the MPIs from the two systems showed moderate agreement levels, with the pelvic angle exhibiting the strongest correlations (ICC: 0.672), followed by the right FAR, left FARQ1, and right LAR (ICC range: 0.608 to 0.669).

Table 2. Descriptive and validity statistics for the MPIs from the 3D motion and LEOMO systems. Data presented are mean ± SD, mean bias [95% LoA], ICC [95% CI], and mean difference [95% CI] from 16 cyclists.

	3D motion (°)	LEOMO (°)	Mean bias (°)	ICC	Mean difference (°)
MPIs	mean ± SD	mean ± SD	[95% LoA]	[95% CI]	[95% CI]
Left FAR	57.06 ± 9.96	53.41 ± 8.66	−3.65 [−23.94, 16.66]	0.41 [−0.09, 0.75]	−3.65 [−9.16, 1.87]
Right FAR	56.00 ± 6.27	52.77 ± 7.17	−3.23 [−14.44, 7.97]	0.67 [0.28, 0.87]	−3.23 [−6.28, −0.18]
Left FARQ1	32.45 ± 5.09	38.02 ± 8.53	5.57 [−6.31, 17.46]	0.66 [0.26, 0.87]	5.57 [2.35, 8.79]
Right FARQ1	34.15 ± 5.41	39.88 ± 8.07	5.73 [−10.83, 22.29]	0.26 [−0.25, 0.66]	5.73 [1.22, 10.23]
Left LAR[1]	46.54 ± 3.52	51.72 ± 7.65	5.18 [−7.83, 18.25]	0.40 [−0.122, 0.748]	5.17 [1.48, 8.87]
Right LAR	51.16 ± 4.24	55.12 ± 5.86	3.96 [−5.24, 13.15]	0.61 [0.18, 0.84]	3.96 [1.46, 6.46]
Pelvic rock	10.48 ± 5.49	5.36 ± 1.25	−5.13 [−16.16, 5.91]	−0.00 [−0.48, 0.48]	−5.13 [−8.13, −2.13]
Pelvic rotation	5.65 ± 4.28	13.60 ± 4.68	7.95 [−5.51, 21.40]	−0.18 [−0.61, 0.33]	7.95 [4.29, 11.60]
Pelvic angle	29.95 ± 10.92	44.58 ± 10.48	14.63 [−3.10, 32.36]	0.67 [−0.28, 0.87]	14.63 [9.81, 19.45]

[1]Data from $n = 15$. Pelvic angle of 0° represents the pelvis being vertical and 90° being horizontal in the sagittal plane. Abbreviations: 3D = three dimensional; CI = confidence interval; FAR = foot angular range; FARQ1 = foot angular range first quadrant; ICC = intraclass correlation coefficient; LAR = leg angular range; LoA = limits of agreement; MPIs= motion performance indicators; SD = standard deviation.

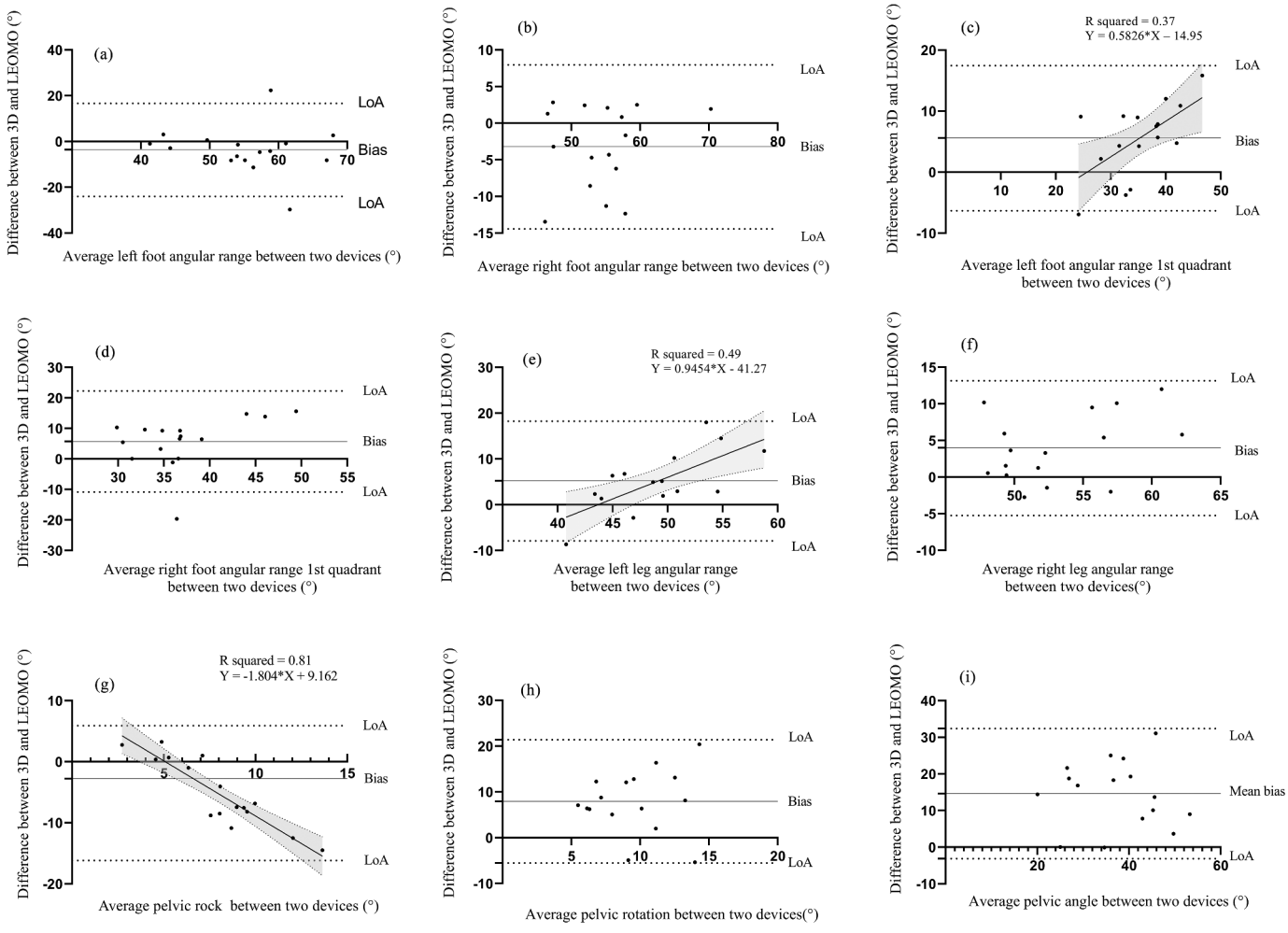

Figure 3. Bland-Altman plots. The x-axis displays the average of the 3D and LEOMO data. The y-axis displays the difference between the two systems. The mean bias and 95% limits of agreement (LoA), and the confidence intervals are also presented. (a) Left foot angular range (FAR). (b) Right FAR. (c) Left foot angular range first quadrant (FARQ1), 12 to 3 o'clock. (d) Right FARQ1, 12 to 3 o'clock. (e) Left leg angular range (LAR). (f) Right LAR. (g) Pelvic rock. (h) Pelvic rotation. (i) Pelvic angle.

The Bland-Altman plots are provided in Figure 3 for the nine MPIs. The left FARQ1 (Figure 3(c)), left LAR (Figure 3(e)), and pelvic rock (Figure 3(g)) were homoscedastic. As the average values increased, the difference between systems increased for the left FARQ1 and left LAR, but it decreased for the pelvic rock.

Table 3. Change in MPIs between the highest and lowest peak power cycling trial. Data are mean ± SD values from 16 cyclists. Asterisk (*) indicates significant correlations between change in peak power output and change in MPIs.

MPIs	3D motion mean ± SD	LEOMO mean ± SD
Left FAR (°)	0.06 ± 5.45	0.97 ± 8.68
Right FAR (°)	1.45 ± 6.64*	1.03 ± 2.63
Left FARQ1 (°)	0.85 ± 3.09	2.85 ± 7.32
Right FARQ1 (°)	1.36 ± 5.21*	2.78 ± 4.59
Left LAR[1] (°)	1.64 ± 2.59	−0.25 ± 4.86
Right LAR (°)	0.50 ± 3.82	2.58 ± 6.14
Pelvic rock (°)	1.21 ± 6.06	0.21 ± 1.61
Pelvic rotation (°)	1.96 ± 3.27	1.14 ± 2.33*
Pelvic angle (°)	2.77 ± 8.13	0.90 ± 3.63

*Data from $n = 15$. The mean change in peak power and SD for 15 cyclists = 96.33 ± 49.63 W. Abbreviations: 3D = three-dimensional; FAR = foot angular range; FARQ1 = foot angular range first quadrant; LAR = leg angular range; MPIs = motion performance indicators; SD = standard deviation.

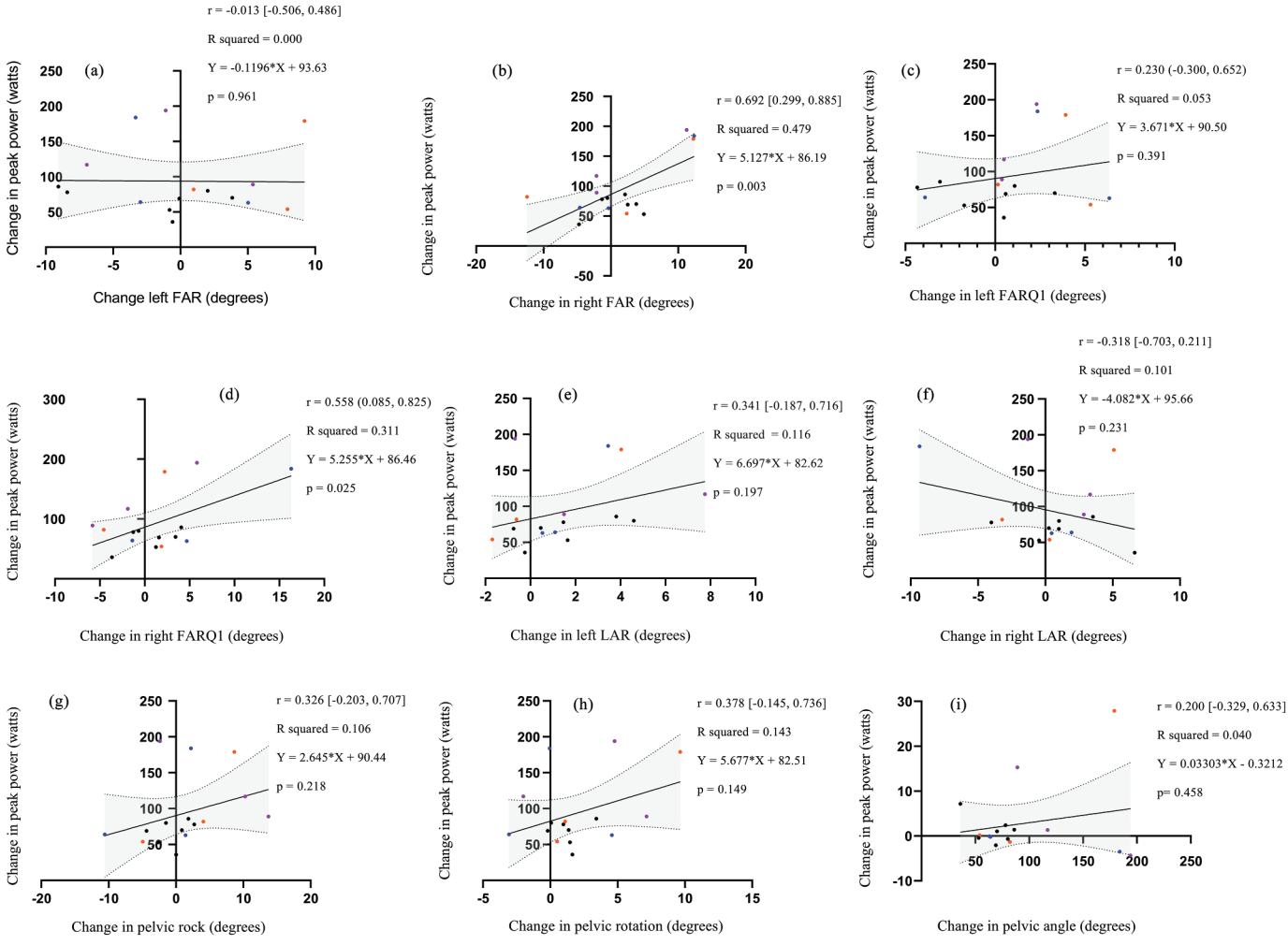

Figure 4. Linear regression plots of the change in peak power between the highest and lowest trials versus the change in the motion performance indicators from the three-dimensional motion system. Pearson correlation values (r) with 95% confidence intervals [lower, upper] and associated p values are provided. The linear regression equation and variance explained (R squared) are also shown. Male elite cyclists (black), female elite cyclists (orange), male junior cyclist (blue), and female junior cyclists (purple) are shown. (a) Left foot angular range (FAR). (b) Right foot FAR. (c) Left foot angular range first quadrant (FARQ1), 12 to 3 o'clock. (d) Right FARQ1, 12 to 3 o'clock. (e) Left leg angular range (LAR). (f) Right LAR. (g) Pelvic rock. (h) Pelvic rotation. (I) Pelvic angle.

Relationship between kinematics and peak power output

The exploratory analyses of the relationship between the change in peak power and the change in MPIs for the 3D and LEOMO data are presented in Table 3. The mean difference in peak power between the highest and lowest cycling trials was 93.63 ± 49.16 W for the 16 cyclists. Figures 4 and 5 present the Pearson correlation and linear regression analyses performed on the 3D and LEOMO data, respectively. Two of the 3D MPIs

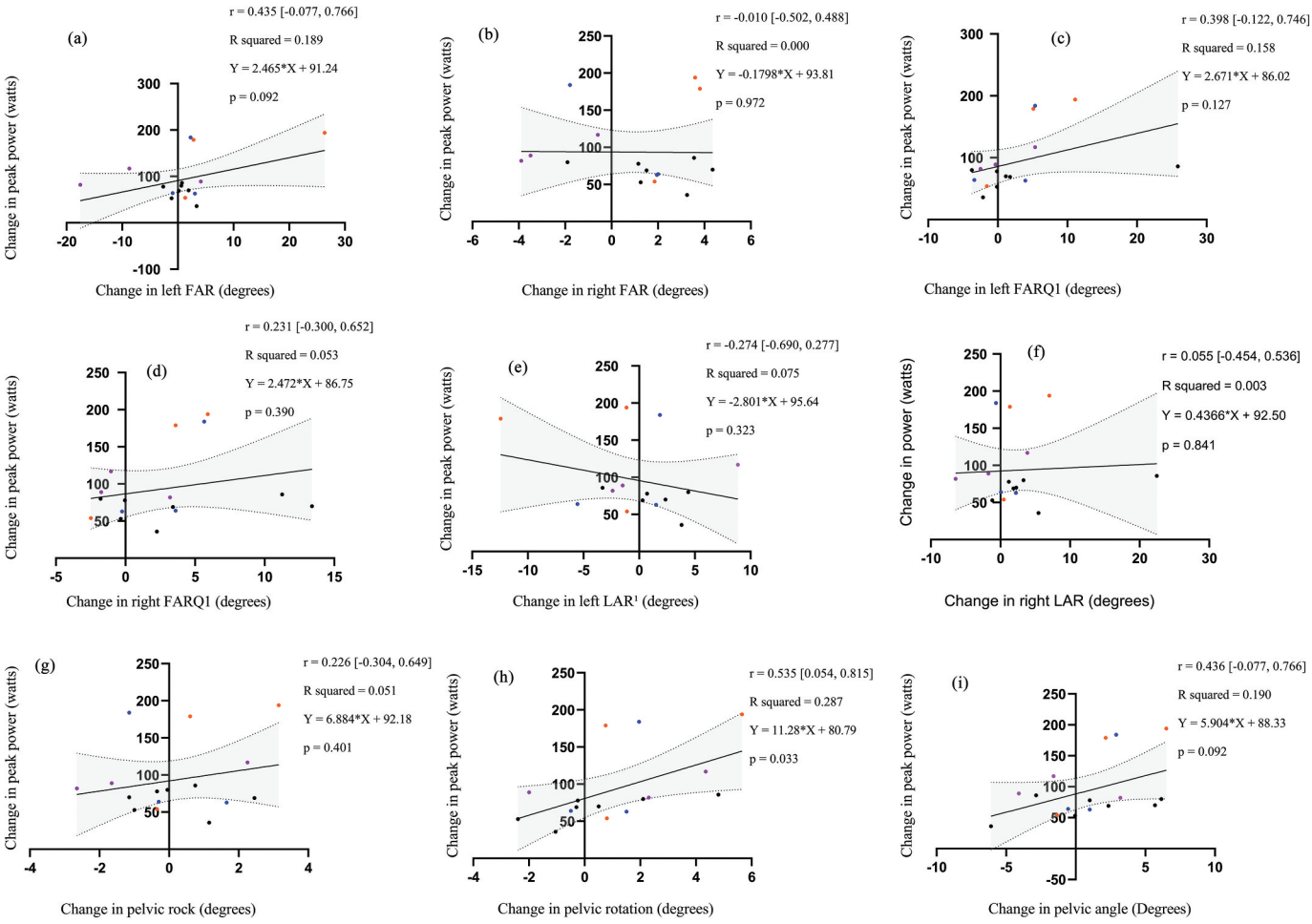

Figure 5. Linear regression plots of the change in peak power between the highest and lowest trials versus the change in the motion performance indicators from the LEOMO device. Pearson correlation values (*r*) with 95% confidence intervals [lower, upper] and associated *p* values are provided. The linear regression equation and variance explained (R squared) are also shown. Male elite cyclists (black), female elite cyclists (orange), male junior cyclist (blue), and female junior cyclists (purple) are shown. (a) Left foot angular range (FAR). (b) Right foot FAR. (c) Left foot angular range first quadrant (FARQ1), 12 to 3 o'clock. (d) Right FARQ1, 12 to 3 o'clock. (e) Left leg angular range (LAR), data from $n = 15$. (f) Right LAR. (g) Pelvic rock. (h) Pelvic rotation. (i) Pelvic angle.

showed large significant correlations to change in peak power: right FARQ1 ($p = 0.025$) and right FAR ($p = 0.003$). Pelvic rotation ($p = 0.033$) was the only large significant correlation with change in peak power for the LEOMO MPIs. All other relationships explored were not significant.

Discussion

We hypothesised that the LEOMO TYPE-S would be a valid tool for measuring kinematics in 3D planes during short maximal sprints with track cyclists, and possibly pave the way forward in obtaining kinematic data on the track. However, our findings suggest the LEOMO-derived MPIs were not valid when compared to gold-standard 3D motion capture in laboratory. At best, four MPIs from the LEOMO demonstrated moderate agreement with the 3D data, with the pelvic angle having the strongest agreement (ICC = 0.672), and the remaining five MPIs exhibiting poor agreement.

Clinical validation of IMUs is seldom performed (Routhier et al., 2020), even though independent validity and reliability testing of IMUs in sport-specific conditions is encouraged (Hughes et al., 2021). A previous validation study compared LEOMO-derived MPIs against 2D data collected over two 6-minute steady-state cycling bouts on a cycling ergometer (Plaza-Bravo et al., 2022), which is not applicable to sprint cycling. Overall, this prior validation study found higher agreement levels between the MPIs collected from the LEOMO and 2D system than ours. Notably, agreement levels between systems were excellent for the FARQ1 and FAR (ICC = 0.88–0.97), and moderate for the LAR and pelvic angles (ICC = 0.52–0.71) (Plaza-Bravo et al., 2022). These findings contrast with ours where only four MPIs showed moderate levels of relative agreement with the 3D motion system, and none showed excellent agreement. In both studies, the LEOMO overestimated pelvic angles by approximately 15° (Plaza-Bravo et al., 2022).

Overall, our findings discourage use of the LEOMO device for assessing sprint cycling kinematics during short maximal efforts from a static position. We do not know if the LEOMO applies a static offset correction, which might be different for right and left sides or different segments. This offset would influence systematic errors, but it does not help in controlling random errors. Indeed, our data collection started from a static seated

position and lasted 15 s. Inspection of the LEOMO files indicate the sensors were unable capturing data from the first pedal cycle. Although this limitation did not impact the data used for analysis (i.e., five pedal cycles prior to cyclists reaching their peak cadence), the LEOMO device may be better suited for longer steady-state cycling efforts, as advanced elsewhere (Plaza-Bravo et al., 2022).

The LEOMO system defines pelvic angle in relation to vertical (LEOMO Help Centre, 2020b), with no measure truly reflecting hip flexion. On the velodrome, bikes are seldom vertical. Hence, further validation for the pelvic angle MPI is required for use on the velodrome. Ideally, algorithms would be developed and validated to enable calculations of hip flexion angles as these are important for aerodynamic positioning on the bike (Faulkner & Jobling, 2021) and managing hip pain in cyclists, which are common in elite cyclists (Baron et al., 2018).

This study used 3D motion capture as the gold standard, which also have limitations. It is well recognised that soft tissue artefact occurs between the bone or skin and markers (Shultz et al., 2011). Five clusters were used to reduce individual marker skin movement artefacts (Cappozzo et al., 1997). Furthermore, the positioning of the LEOMO sensors and the 3D markers between cyclists may have been inconsistent, possibly contributing to the differences between systems. The same experienced physiotherapist positioned all LEOMO sensors and reflective markers to limit the effect of marker and sensor placement on outcomes.

As proposed in other research papers (R. Bini & Hunter, 2023; Courel-Ibáñez et al., 2021; Faulkner & Jobling, 2021; Jongerius et al., 2022), specific biomechanics can influence performance or help mitigate or manage injury within cycling. Our exploration of potential relationships between changes in peak power and changes in MPIs indicated that only two MPIs from the 3D kinematics (right FARQ1 and right FAR) and one from the LEOMO (pelvic rotation) were largely and significantly correlated with changes in peak power. Increases in these MPI values were linked to an increase in peak power. Our findings that a greater range of motion at the right foot is linked to an increase in peak power from the 3D analysis contradicts findings from a prior study (Courel-Ibáñez et al., 2021) where, using an IMU sampling at 100 Hz, the authors identified that less range of motion of the right foot was associated with greater peak power in professional cyclists in a graded exercise test. Our study differed in that it measured maximum cycling intensity from a static seated position, quickly reaching a very high peak power, versus a graded exercise test. The sudden increase in peak power and significant forces required to initiate torque from static starts may require more ankle stability versus a graded exercise test. The inability to maintain ankle stability during starts may explain the positive correlation between peak power and increased foot range of movement in our study. Most of the riders started with their non-dominant leg (left leg), which could also contribute to the asymmetry in ankle range of motion and reason why only the right FAR and right FARQ1 was positively associated with peak power. The difference between studies may also be due to differences in equipment used to derive MPIs, i.e., 3D motion versus IMU. Our current study indicated only moderate levels of agreement between 3D and IMUs for right FAR. Speculatively, in our cohort, only the right foot range of motion was linked to a change in peak power due to track cyclists always riding clockwise and the right leg being the dominant leg.

Elite athletes are better at varying their kinematics to meet specific performances during stable tasks. This kinematic adaptability may be advantageous to minimise the effects of fatigue or the environment (Cowin et al., 2022), for instance. Our cohort showed small changes in 3D kinematics between their highest and lowest peak power trials (0.06° to 2.77°), which would make establishing relationships between kinematics and performance changes difficult. Nonetheless, the relatively larger SD values (2.59° to 8.13°) suggest kinematic variability between cyclists (Table 3). Furthermore, the heterogeneity of our cohort will increase the variability in cycling biomechanics due to differences in their metabolic and muscular capacities (Elmer et al., 2011). Albeit all high-level track cyclists, our cohort was varied and included juniors, elite, males, and females. Assessing kinematics with this heterogeneity cohort can make validation and correlation studies challenging.

Conclusion

Given our findings, use of the LEOMO motion sensor device for track cyclists in this specific setting is discouraged. This device may be more suitable for steady-state cycling monitoring and needs further development before use in sprint track cycling. Our exploratory analysis indicates that there may be value in greater right foot angular range and right foot angular range first quadrant for peak power generation in short sprint efforts from a seated position, although causality has not here been explored.

Confirmation of ethical compliance

The Human Research Ethics Committee Application HREC(HECS)2022 #06.

Acknowledgments

The authors would like to thank the support from Cycling New Zealand and all cyclists participating in this study.

Disclosure statement

No potential conflict of interest was reported by the author(s).

Funding

Prime Minister's Support Scholarship | HPSNZ.

ORCID

Roné Thompson http://orcid.org/0009-0006-4292-1125

References

Baron, H., Reid, D., & Hamilton, B. (2018). Injury surveillance in elite New Zealand track cyclists: Establishing the baseline incidence and prevalence of injury and its effect on training and competition for elite new zealand cyclists. *New Zealand Journal of Sports Medicine*, *45*(1), 12–21.

Benoit, D. L., Ramsey, D. K., Lamontagne, M., Xu, L., Wretenberg, P., & Renstrom, P. (2006). Effect of skin movement artifact on knee kinematics during gait and cutting motions measured in vivo. *Gait & Posture*, *24*(2), 152–164. https://doi.org/10.1016/j.gaitpost.2005.04.012

Benson, L. C., Raisanen, A. M., Clermont, C. A., & Ferber, R. (2022). Is this the real life, or is this just laboratory? A scoping review of imu-based running gait analysis. *Sensors*, *22*(5), 1722. https://doi.org/10.3390/s22051722

Bernardina, G. R. D., Monnet, T., Cerveri, P., Silvatti, A. P., & Ahamed, N. U. (2019). Moving system with action sport cameras: 3D kinematics of the walking and running in a large volume. *PLoS One*, *14*(11), e0224182. https://doi.org/10.1371/journal.pone.0224182

Bertucci, W., Taiar, R., & Grappe, F. (2005). Differences between sprint tests under laboratory and actual cycling conditions. *The Journal of Sports Medicine and Physical Fitness*, *45*(3), 277–283.

Bini, R., Encarnacion-Martinez, A., Priego-Quesada, J. I., & Carpes, F. P. (2023). Details our eyes cannot see: Challenges for the analysis of body position during bicycle fitting. *Sports Biomechanics*, *22*(4), 485–493. https://doi.org/10.1080/14763141.2021.1987509

Bini, R., & Hunter, J. R. (2023). Pain and body position on the bicycle in competitive and recreational road cyclists: A retrospective study. *Sports Biomechanics*, *22*(4), 522–535. https://doi.org/10.1080/14763141.2021.1942967

Bini, R. R., Dagnese, F., Rocha, E., Silveira, M. C., Carpes, F. P., & Mota, C. B. (2016). Three-dimensional kinematics of competitive and recreational cyclists across different workloads during cycling. *European Journal of Sport Science*, *16*(5), 553–559. https://doi.org/10.1080/17461391.2015.1135984

Bishop, D. (2008). An applied research model for the sport sciences. *Sports Medicine*, *38*(3), 253–263. https://doi.org/10.2165/00007256-200838030-00005

Bland, J. M., & Altman, D. G. (1999). Measuring agreement in method comparison studies. *Statistical Methods in Medical Research*, *8*(2), 135–160. https://doi.org/10.1177/096228029900800204

Brito, J., Lopes, L., Conceição, A., Costa, A. M., & Louro, H. (2014). Stationary roller versus velodrome for maximal cycling test: A comparison. *Journal of Human Sport & Exercise*, *9*(1), 7–16. https://doi.org/10.4100/jhse.2014.91.02

Brocherie, F., & Dinu, D. (2022). Biomechanical estimation of tennis serve using inertial sensors: A case study. *Frontiers in Sports and Active Living*, *4*, 4. https://doi.org/10.3389/fspor.2022.962941

Burnie, L. (2020). *The Effects of Strength Training on Intermuscular Coordination* [Doctoral dissertation, Sheffield Hallam University]. http://shura.shu.ac.uk/27025/

Burnie, L., Barratt, P., Davids, K., Worsfold, P., & Wheat, J. (2023). Biomechanical measures of short-term maximal cycling on an ergometer: A test-retest study. *Sports Biomechanics*, *22*(8), 997–1015. https://doi.org/10.1080/14763141.2020.1773916

Cappozzo, C. A., Croce, U., Pensalfini, F., & Pensalfini, F. (1997). Surface-marker cluster design criteria for 3-D bone movement reconstruction. *IEEE Transactions on Biomedical Engineering*, *44*(12), 1165–1174. https://doi.org/10.1109/10.649988

Catelli, D. S., Wesseling, M., Jonkers, I., & Lamontagne, M. (2019). A musculoskeletal model customized for squatting task. *Computer Methods in Biomechanics and Biomedical Engineering*, *22*(1), 21–24. https://doi.org/10.1080/10255842.2018.1523396

Chambers, R., Gabbett, T. J., Cole, M. H., & Beard, A. (2015). The use of wearable microsensors to quantify sport-specific movements. *Sports Medicine*, *45*(7), 1065–1081. https://doi.org/10.1007/s40279-015-0332-9

Cohen, J. (1992). A power primer. *Psychological Bulletin*, *112*(1), 155–159. https://doi.org/10.1037/0033-2909.112.1.155

Courel-Ibáñez, J., Mateo-March, M., Moreno-Pérez, V., & Bini, R. (2021). Sensitivity of cycling motion performance indicators (MPIs) to incremented load and their relationship with performance in professional cyclists. *Proceedings of the Institution of Mechanical Engineers, Part P: Journal of Sports Engineering & Technology*, 779. https://doi.org/10.1177/17543371211062061

Cowin, J., Nimphius, S., Fell, J., Culhane, P., & Schmidt, M. (2022). A proposed framework to describe movement variability within sporting tasks: A scoping review. *Sports Medicine - Open*, *8*(1), 85. https://doi.org/10.1186/s40798-022-00473-4

Delgado-García, G., Vanrenterghem, J., Ruiz-Malagón, E. J., Molina-García, P., Courel-Ibáñez, J., & Soto-Hermoso, V. M. (2020). IMU gyroscopes are a valid alternative to 3D optical motion capture system for angular kinematics analysis in tennis. *Journal of Sports Engineering and Technology*, *235*(1), 3–12. https://doi.org/10.1177/1754337120965444

Delp, S. L., Anderson, F. C., Arnold, A. S., Loan, P., Habib, A., John, C. T., Guendelman, E., & Thelen, D. G. (2007). Opensim: Open-source software to create and analyze dynamic simulations of movement. *IEEE Transactions on Biomedical Engineering*, *54*(11), 1940–1950. https://doi.org/10.1109/TBME.2007.901024

Elmer, S. J., Barratt, P. R., Korff, T., & Martin, J. C. (2011). Joint-specific power production during submaximal and maximal cycling. *Medicine & Science in Sports & Exercise*, *43*(10), 1940–1947. https://doi.org/10.1249/MSS.0b013e31821b00c5

Faulkner, S. H., & Jobling, P. (2021). The effect of upper-body positioning on the aerodynamic-physiological economy of time-trial cycling. *International Journal of Sports Physiology and Performance*, *16*(1), 51–58. https://doi.org/10.1123/ijspp.2019-0547

Ferguson, H., Harnish, C., Klich, S., Michalik, K., Dunst, A. K., Zhou, T., Chase, J. G., & González-Ravé, J. M. (2023). Power-duration relationship comparison in competition sprint cyclists from 1-s to 20-min. Sprint performance is more than just peak power. *PLoS One*, *18*(5), e0280658. https://doi.org/10.1371/journal.pone.0280658

Ferguson, H. A., Harnish, C., & Chase, J. G. (2021). Using field based data to model sprint track cycling performance. *Sports Medicine - Open*, *7*(1), 20. https://doi.org/10.1186/s40798-021-00310-0

Fonda, B., Sarabon, N., & Li, F. X. (2014). Validity and reliability of different kinematics methods used for bike fitting. *Journal of Sports Sciences*, *32*(10), 940–946. https://doi.org/10.1080/02640414.2013.868919

Frank, R. M., Ukwuani, G., Clapp, I., Chahla, J., & Nho, S. J. (2018). High rate of return to cycling after hip arthroscopy for femoroacetabular impingement syndrome. *Sports Health*, *10*(3), 259–265. https://doi.org/10.1177/1941738117747851

Galindo-Martinez, A., Lopez-Valenciano, A., Albaladejo-Garcia, C., Valles-Gonzalez, J. M., & Elvira, J. L. L. (2021). Changes in the trunk and lower extremity kinematics due to fatigue can predispose to chronic injuries in cycling. *International Journal of Environmental Research and Public Health*, *18*(7), 3719. https://doi.org/10.3390/ijerph18073719

Geoffrey, M., Duc, S., Ouvrard, T., Damien, S., Puel, F., & Bertucci, W. (2020). Variability of ankle kinematics in professional cyclists: Consequence on saddle height adjustment. *Journal of Science and Cycling*, *9*(1), 25–32. https://doi.org/10.28985/0620.jsc.03

Hébert-Losier, K., Yin, N. S., Beaven, C. M., Tee, C. C. L., & Richards, J. (2019). Physiological, kinematic, and electromyographic responses to kinesiology-type patella tape in elite cyclists. *Journal of Electromyography and Kinesiology*, *44*, 36–45. https://doi.org/10.1016/j.jelekin.2018.11.009

Hoon, M. W., Michael, S. W., Patton, R. L., Chapman, P. G., & Areta, J. L. (2016). A comparison of the accuracy and reliability of the wahoo KICKR and SRM power meter. *Journal of Science and Cycling*, *5*(3), 11–15. https://jsc-journal.com/index.php/JSC/article/view/240

Hopkins, W. (2015). Spreadsheets for analysis of validity and reliability. *Sportscience*, *19*, 36–44. https://sportsci.org/2015/ValidRely.htm

Hughes, G. T. G., Camomilla, V., Vanwanseele, B., Harrison, A. J., Fong, D. T. P., & Bradshaw, E. J. (2021). Novel technology in sports biomechanics: Some words of caution. *Sports Biomechanics*, 1–9. https://doi.org/10.1080/14763141.2020.1869453

Hulley, S. B., Cummings, S. R., Browner, W. S., Grady, D. G., & Newman, T. B. (2013). *Designing clinical research: An epidemiologic approach* (4th ed.). Lippincott Williams & Wilkins.

Jongerius, N., Wainwright, B., Walker, J., & Bissas, A. (2022). The biomechanics of maintaining effective force application across cycling positions. *Journal of Biomechanics*, *138*, 111103. https://doi.org/10.1016/j.jbiomech.2022.111103

Koo, T. K., & Li, M. Y. (2016). A guideline of selecting and reporting intraclass correlation coefficients for reliability research. *Journal of Chiropractic Medicine*, *15*(2), 155–163. https://doi.org/10.1016/j.jcm.2016.02.012

Lachin, J. M. (1981). Introduction to sample size determination and power analysis for clinical trials. *Control Clinical Trials*, *2*(2), 93–113. https://doi.org/10.1016/0197-2456(81)90001-5

LEOMO Help Centre. (2020a). *LEOMO*. Retrieved November 1, 2022, from https://leomo.zendesk.com/hc/en-us

LEOMO Help Centre. (2020b). *Pelvic Angle*. Retrieved November 1, 2022, from https://leomo.zendesk.com/hc/en-us

Millour, G., Velásquez, A. T., & Domingue, F. (2022). A literature overview of modern biomechanical-based technologies for bike-fitting professionals and coaches. *International Journal of Sports Science & Coaching*, *18*(1), 292–303. https://doi.org/10.1177/17479541221123960

Nimmerichter, A., & Williams, C. A. (2015). Comparison of power output during ergometer and track cycling in adolescent cyclists. *Journal of Strength and Conditioning Research*, *29*(4), 1049–1056. https://doi.org/10.1519/JSC.0000000000000723

Phillips, K. E., & Hopkins, W. G. (2020). Determinants of cycling performance: A review of the dimensions and features regulating performance in elite cycling competitions. *Sports Medicine - Open*, *6*(1), 23. https://doi.org/10.1186/s40798-020-00252-z

Picerno, P. (2017). 25 years of lower limb joint kinematics by using inertial and magnetic sensors: A review of methodological approaches. *Gait & Posture*, *51*, 239–246. https://doi.org/10.1016/j.gaitpost.2016.11.008

Plaza-Bravo, J. M., Mateo-March, M., Sanchis-Sanchis, R., Perez-Soriano, P., Zabala, M., & Encarnacion-Martinez, A. (2022). Validity and reliability of the leomo motion-tracking device based on inertial measurement unit with an optoelectronic camera system for cycling pedaling evaluation. *International Journal of Environmental Research and Public Health*, *19*(14), 8375. https://doi.org/10.3390/ijerph19148375

Portney, L. G. (2020). *Foundation of clinical research: Applications to evidence-based practice* (4th ed.). F.A. Davis Ltd inc. https://fadavispt.mhmedical.com/content.aspx?bookid=2885§ionid=243179474

Pouliquen, C., Nicolas, G., Bideau, B., & Bideau, N. (2020). Impact of power output on muscle activation and 3D kinematics during an incremental test to exhaustion in professional cyclists. *Frontiers in Sports and Active Living*, *2*, 516911. https://doi.org/10.3389/fspor.2020.516911

Routhier, F., Duclos, N. C., Lacroix, E., Lettre, J., Turcotte, E., Hamel, N., Michaud, F., Duclos, C., Archambault, P. S., Bouyer, L. J., & Papa, F. (2020). Clinicians' perspectives on inertial measurement units in clinical practice. *PLoS One*, *15*(11), e0241922. https://doi.org/10.1371/journal.pone.0241922

Shultz, R., Kedgley, A. E., & Jenkyn, T. R. (2011). Quantifying skin motion artifact error of the hindfoot and forefoot marker clusters with the optical tracking of a multi-segment foot model using single-plane fluoroscopy. *Gait & Posture*, *34*(1), 44–48. https://doi.org/10.1016/j.gaitpost.2011.03.008

Slawinski, J., Louis, J., Poli, J., Tiollier, E., Khazoom, C., & Dinu, D. (2018). The effects of repeated sprints on the kinematics of 3-point shooting in basketball. *Journal of Human Kinetics*, *62*(1), 5–14. https://doi.org/10.1515/hukin-2017-0156

Van der Kruk, E., & Reijne, M. M. (2018). Accuracy of human motion capture systems for sport applications; state-of-the-art review. *European Journal of Sport Science*, *18*(6), 806–819. https://doi.org/10.1080/17461391.2018.1463397

Wadsworth, D. J. S., & Weinrauch, P. (2019). The role of a bike fit in cyclists with hip pain. A clinical commentary. *The International Journal of Sports Physical Therapy*, *14*(3), 468–486. https://doi.org/10.26603/ijspt20190468

Williams, S. J., & Kendall, L. R. (2007). A profile of sports science research (1983–2003). *Journal of Science and Medicine in Sport*, *10*(4), 193–200. https://doi.org/10.1016/j.jsams.2006.07.016